Eur. Phys. J. D **44**, 1–8 (2007)
DOI: 10.1140/epjd/e2007-00141-6

THE EUROPEAN PHYSICAL JOURNAL D

The ground state and doubly-excited $^{1,3}P^{\circ}$ states of hot-dense plasma-embedded Li^+ ions

S. Kar[a] and Y.K. Ho

Institute of Atomic and Molecular Sciences, Academia Sinica, P.O. Box 23-166, Taipei 106, Taiwan

Received 10 November 2006 / Received in final form 20 January 2007
Published online 6 April 2007 –

Abstract. We have investigated the ground state and the doubly excited $^{1,3}P^{\circ}$ resonance states of plasma-embedded Li^+ ion. The plasma effect is taken care of by using a screened Coulomb potential obtained from the Debye model. A correlated wave function has been used to represent the correlation effect between the charged particles. The ground state of Li^+ in plasmas for different screening parameters has been estimated in the framework of Rayleigh-Ritz variational principle. In addition, a total of 18 resonances (9 each for $^1P^{\circ}$ and $^3P^{\circ}$ states) below the $n = 2$ Li^+ thresholds has been estimated by calculating the density of states using the stabilization method. For each spin state, this includes four members in the $2snp_+$ $(2 \leq n \leq 5)$ series, three members in the $2snp_-$ $(3 \leq n \leq 5)$ series, and two members in the $2pnd$ $(n = 3, 4)$ series. The resonance energies and widths for various Debye parameters ranging from infinity to a small value for these $^{1,3}P^{\circ}$ resonance states along with the ground state energies of Li^+ and the Li^{2+} (1S), Li^{2+} (2S) threshold energies are reported. Furthermore, the wavelengths for the photo-absorption of lithium ion from its ground state to such $^1P^{\circ}$ resonance states for different Debye lengths are also reported.

PACS. 52.20.Fs Electron collisions – 95.30.Dr Atomic processes and interactions – 34.80.Bm Elastic scattering of electrons by atoms and molecules – 95.75.Fg Spectroscopy and spectrophotometry

1 Introduction

With the recent advancement for laser plasmas in laser fusion laboratories [1] and with the recent experimental development on the doubly excited resonances in photo-ionization spectrum of Li^+ using the photon-ion merged-beam endstation at the Advanced Light Source [2], it is of interest to investigate the bound states and resonance states of Li^+ under the influence of external environments produced by the charge-neutral background such as that of a plasma. The plasma effect can be represented by different models of screened Coulomb potentials. In hot-dense and low-density warm plasma, the effect of plasma on the localized two-particle interaction can be represented by a screened Coulomb potential obtained from the Debye shielding approach in which the screening parameter μ is proportional to $\sqrt{n/T}$, n being the plasma density and T its temperature, and with $\mu = 1/D$, D being the Debye lengths. Recently, several studies have been performed on the bound states ([3–11], references therein), the resonance states [9,12,13] and other structural properties ([4,7,11,14] and references therein) of two-electron atoms/ions immersed in plasmas by considering the Debye screening concept of plasma modeling. The importance of Debye screening in plasma spectroscopy, in plasma diagnostics, in astrophysical applications and in calculating partition function in thermodynamics and several other applications has been discussed in the literature ([3–17], references therein).

In the present work, we report results for the ground state and the $2ln'l'$ $(2 \leq n' \leq 5)$ $^{1,3}P^{\circ}$ resonances of Li^+ in plasmas below the Li^{2+}(2S) threshold, along with the wavelengths of the absorption resonances in the Li^+ for various Debye lengths using 600-term of a highly correlated exponential basis function. Interaction between the charged particles is taken care of by using the Debye model. We use the stabilization method [18–20] to extract resonance energies and widths. The convergence of the calculations is examined with increasing number of terms and different sets of non-linear variational parameters in the basis expansion. To the best of our knowledge, the investigation on the $^{1,3}P^{\circ}$ resonances of Li^+ in plasmas has not been reported in the literature until now. The ground state energies obtained from our calculations for different screening parameters are lower than the reported results of Saha et al. [6]. The atomic unit (a.u.) has been used throughout the present work.

2 Calculations

The non-relativistic Hamiltonian describing the Li^+ ion embedded in Debye plasmas characterized by a parameter

[a] e-mail: skar@pub.iams.sinica.edu.tw

D, called the Debye length, is given by

$$H = -\frac{1}{2}\nabla_1^2 - \frac{1}{2}\nabla_2^2 - 3\left[\frac{\exp(-r_1/D)}{r_1} + \frac{\exp(-r_2/D)}{r_2}\right] + \frac{\exp(-r_{12}/D)}{r_{12}}, \quad (1)$$

where r_1 and r_2 are the radial coordinates of the two electrons and r_{12} is their relative distance. A set of plasma condition can be simulated for different choice of μ, as the Debye screening parameter μ is a function n and T. Also, it can be observed from the perturbation theory that the screening is repulsive perturbation for which all the isolated energy levels displaced upwards and ultimately in the continuum due to repulsive perturbation.

For the S, P states of Li^+ ion, we have considered the wave function

$$\Psi = (1 + S_{pn}\hat{O}_{21}) \sum_{i=1}^{N} C_i r_1^L P_L(\cos\theta_1) \times \exp\left[(-\alpha_i r_1 - \beta_i r_2 - \gamma_i r_{12})\omega\right] \quad (2)$$

where $\alpha_i, \beta_i, \gamma_i$ are the non-linear variation parameters, C_i $(i = 1, ..., N)$ are the linear expansion coefficients, $L = 0$ for S-states and $L = 1$ for P-states, $S_{pn} = 1$ denotes singlet states and $S_{pn} = -1$ indicates triplet states, N is the number basis terms, and ω is a scaling constant to be discussed later in the text. The operator $\hat{O}_{21}$ is the permutation of the two-identical particles. The non-linear variational parameters α_i, β_i and γ_i are chosen from a quasi-random process as proposed by Frolov [21] and as used in our earlier work [9,11,12,14]. According to the multi-box strategy [21], the parameters α_i, β_i and γ_i are chosen from the three positive interval $[A_1^{(k)}, A_2^{(k)}]$, $[B_2^{(k)}, B_2^{(k)}]$ and $[C_1^{(k)}, C_2^{(k)}]$; where, $k = \mathrm{mod}(i, 3) + 1$, $1 \le i \le N$,

$$\begin{aligned}
\alpha_i &= \eta_1^{(k)}[\langle\langle(i(i+1)\sqrt{2})/2\rangle\rangle(A_2^{(k)} - A_1^{(k)}) + A_1^{(k)}] \\
\beta_i &= \eta_2^{(k)}[\langle\langle(i(i+1)\sqrt{3})/2\rangle\rangle(B_2^{(k)} - B_1^{(k)}) + B_1^{(k)}] \\
\gamma_i &= \eta_3^{(k)}[\langle\langle(i(i+1)\sqrt{5})/2\rangle\rangle(C_2^{(k)} - C_1^{(k)}) + C_1^{(k)}], \quad (3)
\end{aligned}$$

where the symbol $\langle\langle \ldots \rangle\rangle$ designates the fractional part of a real number. The positive scaling factors $\eta_1^{(k)}$, $\eta_2^{(k)}$ and $\eta_3^{(k)}$ are set to have values equal to 1 in the first stage, and in the second stage they will be varied. But for the present investigation, it has been observed that a better optimization can be obtained by selecting $A_1^{(k)} = 0$, $A_2^{(k)} = a$; $B_1^{(k)} = 0$, $B_2^{(k)} = b$; $C_1^{(k)} = 0$, $C_2^{(k)} = c$. For the ground state calculation, the optimum values for a and b are 4.1 and 5.2 respectively for all Debye lengths. The optimum value of c is the same for Debye lengths up to $D = 0.6$ and the value is 4.7. The optimized values of c are 1.2, 0.3, 0.3 and 0.2 for $D = 0.5$, 0.4, 0.3, and 0.29, respectively. For P-state calculations, the optimized values for a, b and c are 3.1, 4.3 and 3.3 respectively for all Debye lengths. The small variation on the non-linear parameters in the neighborhood of the optimized value does not affect significantly on the best energies.

Table 1. Ground state energies (in a.u.) for plasma-embedded Li^+ and Li^{++}.

D	$Li^+(1s^2\ ^1S)$	$Li^{2+}(1S)$
∞	−7.2799134126	−4.5000000000
	−7.2799134127[a]	(exact)
100	−7.2300418387	−4.4700748341
	−7.2299475[b]	
50	−7.1804259670	−4.4402986787
20	−7.0330957201	−4.3518546295
10	−6.7925067101	−4.2073405204
	−6.7924170[b]	
5	−6.3292677550	−3.9287753707
3	−5.7469045658	−3.5779433744
2.5	−5.4700821388	−3.4109051746
2	−5.0719624391	−3.1703316413
1.5	−4.4519157903	−2.7947384167
1.0	−3.3626607029	−2.1314940324
	−3.3612769[b]	
0.6	−1.7144175621	−1.1143173063
0.5	−1.123070158	−0.742026070
	−1.0911718[b]	
0.4	−0.49078398	−0.33460641
0.3	−0.02158	−0.01582
	0.076012[b]	
0.29	−0.0056	−0.0042

[a] Reference [22]; [b] reference [6].

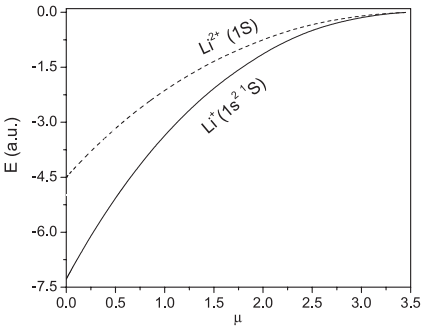

Fig. 1. The ground state energies of Li^+ in terms of Debye screening parameter μ along with the Li^{2+} (1S) thresholds.

3 Ground state of Li^+ immersed in Debye plasmas

For the ground state calculation of Li^+ ion we first set $\omega = 1$ in equation (2). To obtain the ground state energies of plasma-embedded Li^+ ion, we first obtain the solution of $H\Psi = E\Psi$, where $E < 0$ in the framework of Rayleigh-Ritz variational principle. The optimum values of the non-linear variational parameters α_i, β_i and γ_i are selected form the quasi-random process [21] in equation (3) to achieve a minimum energy for each screening parameter. We have estimated the ground $1s^2\ ^1S$ state of Li^+ in plasmas for different Debye lengths and the results are presented in Table 1 for different Debye lengths, D and in Figure 1 as functions of Debye screening parameters, μ. In the unscreened case our results compare well with the best results in the literature [22]. For the screened cases, our calculated ground state energy values are lower than the reported results of Saha et al. [6]. A comparison is made

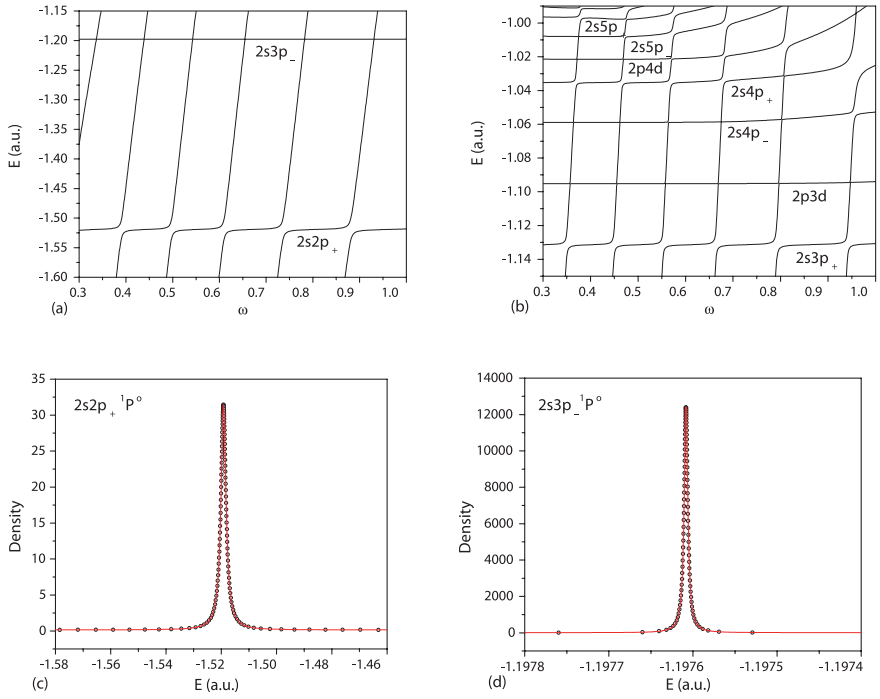

Fig. 2. The stabilization diagram of $2ln'l'$ $(2 \le n' \le 5)$ ^{1}P° resonances in (a) and (b) along with the fittings (solid line) of the calculated density of states (circles) for the $2s2p_+$ ^{1}P° state in (c) and the $2s3p_-$ ^{1}P° state in (d) of Li^+ in plasmas for $D = 20$.

in Table 1. In Table 1 and Figure 1, we also present the Li^{2+}(1S) threshold energies. The Li^{2+} (1S) and Li^{2+} (2S) threshold energies have been calculated by diagonalizing the standard Slater-type orbitals and our results compare well with the available results in the literature [23].

It is clear from Table 1 and Figure 1 that the ground state energies of Li^+ in plasmas for different shielding parameters are very close to the Li^{2+} (1S) threshold energies with the increase of plasma strength i.e., increase of the Debye screening parameter μ. Our final results are obtained using 600-term basis functions (2), but we have also tested that the ground state energies produce the same accuracy as presented in Table 1 using 700-term basis functions.

4 The ^{1,3}P° resonance states of Li^+ immersed in Debye plasmas

To calculate ^{1,3}P° resonances using stabilization method [18–20], we compute the energy levels $E(\omega)$ for different Debye lengths by diagonalizing the Hamiltonian (1) with basis function (2) using the appropriate choice of the non-linear parameters α_i, β_i, γ_i which yield the best bound ^{1,3}P° states energies and the varying scaling factor ω in the range of 0.3–1.0 with a mesh size 0.001. We then construct the stabilization diagrams (as shown in Figs. 2a and 2b) by plotting $E(\omega)$ versus ω. The stabilized or slowly varying energy levels appear in the stabilization plateau indicates the position of the resonance at an energy E. The details of successful applications of this simple and powerful method are available in the works of Ho and co-workers ([9,12,18–20] and references therein). Varying the Debye length D from infinity to small values, different resonance parameters (energies and widths) are obtained for various Debye lengths.

To extract the resonance energy E_r and the resonance width Γ for a particular resonance, we calculate the density of resonance states for a single energy level using the formula [19,20],

$$\rho_n(E) = \left| \frac{E_n(\omega_{i+1}) - E_n(\omega_{i-1})}{\omega_{i+1} - \omega_{i-1}} \right|^{-1}_{E=E_n(\omega_i)}, \qquad (4)$$

where the index i is the ith varied ω value, i.e., ω_i and the index n is for the nth resonance. Also in equation (4), ω_{i-1} and ω_{i+1} are respectively the $(i-1)$th and $(i+1)$th varied ω values next to ω_i. After calculating the density of resonance states $\rho_n(E)$ using formula (4), we fit it to the following Lorentzian form that yields resonance energy E_r and a total width Γ, with

$$\rho_n(E) = y_0 + \frac{A}{\pi} \frac{(\Gamma/2)}{(E - E_r)^2 + (\Gamma/2)^2}, \qquad (5)$$

where y_0 is the baseline offset, A is the total area under the curve, E_r is the center of the peak, and Γ denotes the full width of the peak of the curve at half height. We should mention here that equation (4) is a modification of the original formula proposed by Mandelshtam et al. [18] in which an averaged form of the density of resonance states was reported. In our earlier works ([12,19,20] and references therein) and in this work, instead of using the averaging formula, we use equation (4) to calculate the density of states for each energy level in the stabilization plateau. The calculated density of states is then fitted to equation (5), and the one that gives the best fit (with the least chi-square and with the best value of the square of the correlation coefficient) to the Lorentzian form is considered as the desired results for that particular resonance.

Table 2. The $^1P^\circ$ resonance energies (E_r in a.u.) in plasmas for various Debye lengths.

D	$2s2p_+$ $^1P^\circ(1)$	$2s3p_+$ $^1P^\circ(3)$	$2s4p_+$ $^1P^\circ(6)$	$2s5p_+$ $^1P^\circ(9)$	Li^{2+} (2S)
∞	−1.757556	−1.361487	−1.255444	−1.2073	−1.1250000000
	−1.75756[a]	−1.36143[a]			
100	−1.708035	−1.312331	−1.206770	−1.1587	−1.0952976996
50	−1.659457	−1.264807	−1.160592	−1.1145	−1.0661818501
40	−1.635515	−1.241636	−1.138377	−1.0933	−1.0518397912
35	−1.618554	−1.225319	−1.122851	−1.0786	−1.0416823893
30	−1.596119	−1.203863	−1.102602	−1.0596	−1.0282508009
25	−1.565052	−1.174386	−1.075018	−1.0338	−1.0096586282
20	−1.519189	−1.131373	−1.035312	−0.9975	−0.9822274203
15	−1.444676	−1.062771	−0.973329	−0.942	−0.9377005540
10	−1.302622	−0.936486	−0.8636		−0.8529472079
7	−1.132966	−0.793889			−0.7519442118
5	−0.928064	−0.63538			−0.6302120452
4	−0.767523				−0.5349233591
3	−0.536306				−0.3973939799
2.5	−0.382279				−0.3049246036
2	−0.201453				−0.1926416821
D	$2s3p_-$ $^1P^\circ(2)$	$2s4p_-$ $^1P^\circ(5)$	$2s5p_-$ $^1P^\circ(8)$	2p3d $^1P^\circ(4)$	2p4d $^1P^\circ(7)$
∞	−1.430517	−1.282427	−1.22085	−1.325190	−1.24072
	−1.4305175[a]			−1.325188[a]	
100	−1.381233	−1.233582	−1.17256	−1.276035	−1.19209
50	−1.333346	−1.186933	−1.12742	−1.228519	−1.14603
40	−1.309911	−1.164387	−1.10592	−1.205351	−1.12391
35	−1.293375	−1.148587	−1.09098	−1.189039	−1.10845
30	−1.271586	−1.127907	−1.07156	−1.167588	−1.08828
25	−1.241574	−1.099674	−1.04531	−1.138121	−1.06086
20	−1.197608	−1.058842	−1.0078	−1.095127	−1.02145
15	−1.127051	−0.994618	−0.9505	−1.026576	−0.9601
10	−0.995623	−0.87934		−0.900562	−0.8531
7	−0.844344	−0.7538		−0.760010	
5	−0.671147				
4	−0.544992				

[a]Reference [25].

Here the scaling factor ω acts as the reciprocal range of the "soft" wall [19,20].

The stabilization plots in Figures 2a and 2b show stabilization characteristic near energies $E_r \approx -1.52$, -1.20, -1.13, -1.10, -1.06, -1.03, -1.02, -1.01 and -1.00 a.u., respectively, for the $^1P^\circ$ states. The stabilization diagrams in Figures 2a and 2b are corresponding to $D = 20$ for the $2s2p_+$, $2s3p_-$, $2s3p_+$, $2p3d$, $2s4p_-$, $2s4p_+$, $2p4d$, $2s5p_-$, $2s5p_+$ $^1P^\circ$ resonance states respectively. In the next step of the stabilization method, we calculate the density of states using the formula (4) for the stabilized portions of each energy level for a particular resonance state (e.g. $2s2p_+$) and then the calculated density of states are fitted to the formula (5). Figures 2c and 2d show the density of resonance states corresponding to the energy levels in the stabilization plots shown in Figures 2a and 2b respectively for the $2s2p_+$ and $2s3p_-$ $^1P^\circ$ states. From the fits 2c and 2d, we obtain the resonances parameters (E_r, Γ) as $(-1.519189, 2.179 \times 10^{-3})$ a.u. and $(-1.197608, 5.229 \times 10^{-6})$ a.u., respectively. Similarly, we calculate several $^{1,3}P^\circ$ resonances for various Debye lengths D ranging from infinity to small values (up to 1.7).

Our results for the resonance energy E_r and width Γ are presented in Tables 2–6 and Figures 3, 4; and they are calculated using the 600-term wave functions of equation (2). For the unscreened case, our resonance parameters for the $^{1,3}P^\circ$ states are fairly comparable with the reported results of other theoretical calculations ([2,24,25], references therein), as shown in Tables 2–6 except for the resonance width of the $2s4p_+$ $^1P^\circ$ state. In Tables 5 and 6, we have made a comparison of our estimated $^{1,3}P^\circ$ resonance parameters (E_r, Γ) in eV for the unscreened case, measured from the ground state energies of Li^+ with the available experimental results. The experimental $^1P^\circ$ resonance parameters(E_r, Γ) (reported by Scully et al. [2], and by Mosiner et al. [26], compare well with our calculations (see Tabs. 5 and 6). The resonance width for the $2s4p_+$ $^1P^\circ$ state is higher than the reported theoretical and experimental results. The reduced a.u. for Li is used for energy conversion (1a.u. = 27.20952 eV) in Tables 5, 6.

All together, we have calculated the resonance widths for the $2s2p_+$, $2s3p_+$, $2s4p_+$, $2s3p_-$, $2p3d$ $^1P^\circ$ states and the $2s2p_+$, $2s3p_+$, $2s4p_+$, $2s3p_-$ $^3P^\circ$ states corresponding to the resonance energies given in Tables 2, 3. For the singlet and triplet state cases, the widths for some of the states are not reported, as these widths are very narrow. From Figures 3, 4 and Tables 2–4, it is clear that the resonance energies increase and ultimately are

Table 3. The ^{3}P$^\circ$ resonance energies (E_r in a.u.) in plasmas for various Debye lengths.

D	$2s2p_+$ ^{3}P$^\circ$(1)	$2s3p_+$ ^{3}P$^\circ$(2)	$2s4p_+$ ^{3}P$^\circ$(5)	$2s5p_+$ ^{3}P$^\circ$(8)	Li^{2+} (2S)
∞	−1.878179	−1.406275	−1.274755	−1.2174	−1.1250000000
	−1.878185[a]	−1.40627[a]			
100	−1.828614	−1.357027	−1.225952	−1.1692	−1.0952976996
50	−1.779908	−1.309244	−1.179420	−1.1242	−1.0661818501
40	−1.755873	−1.285885	−1.156957	−1.1028	−1.0518397912
35	−1.738833	−1.269413	−1.141227	−1.0878	−1.0416823893
30	−1.716278	−1.247722	−1.120650	−1.0686	−1.0282508009
25	−1.685016	−1.217869	−1.092584	−1.0426	−1.0096586282
20	−1.638800	−1.174187	−1.052045	−1.0049	−0.9822274203
15	−1.563554	−1.104220	−0.988415	−0.9487	−0.9377005540
10	−1.419529	−0.974367	−0.874709		−0.8529472079
7	−1.246486	−0.825750	−0.75309		−0.7519442118
5	−1.035815	−0.657438			−0.6302120452
4	−0.869230	−0.538273			−0.5349233591
3	−0.626136				−0.3973939799
2.5	−0.461062				−0.3049246036
2	−0.259976				−0.1926416821
1.8	−0.171969				−0.1428292398
1.7	−0.12843				−0.1174318560
D	$2s3p_-$ ^{3}P$^\circ$(3)	$2s4p_-$ ^{3}P$^\circ$(6)	$2s5p_-$ ^{3}P$^\circ$(9)	2p3d ^{3}P$^\circ$(4)	2p4d ^{3}P$^\circ$(7)
∞	−1.398514	−1.26855	−1.2136	−1.33621	−1.24591
	−1.398514[a]			−1.33621[a]	
100	−1.349269	−1.21977	−1.1654	−1.28702	−1.19724
50	−1.301495	−1.17330	−1.1205	−1.23939	−1.15107
40	−1.278142	−1.15089	−1.0991	−1.21614	−1.12885
35	−1.261674	−1.13520	−1.0843	−1.19976	−1.11333
30	−1.239988	−1.11469	−1.0651	−1.17821	−1.09306
25	−1.210141	−1.08670	−1.0391	−1.14858	−1.06547
20	−1.166469	−1.04632	−1.0021	−1.10530	−1.02577
15	−1.096518	−0.98302	−0.9447	−1.03615	−0.96384
10	−0.966743	−0.87012		−0.90856	−0.8548
7	−0.818480			−0.76479	
5	−0.650335				

[a]Reference [24].

Table 4. The ^{1,3}P$^\circ$ resonance widths (Γ in a.u.) of Li^+ under Debye screening.

D	$2s2p_+$ ^{1}P$^\circ$(1) [10^{-3}]	$2s3p_+$ ^{1}P$^\circ$(3) [10^{-4}]	$2s4p_+$ ^{1}P$^\circ$(6) [10^{-4}]	$2s3p_-$ ^{1}P$^\circ$(2) [10^{-6}]	$2p3d$ ^{1}P$^\circ$(4) [10^{-6}]	$2s2p_+$ ^{3}P$^\circ$(1) [10^{-4}]	$2s3p_+$ ^{3}P$^\circ$(2) [10^{-4}]	$2s4p_+$ ^{3}P$^\circ$(5) [10^{-5}]	$2s3p_-$ ^{3}P$^\circ$(3) [10^{-6}]
∞	2.212	6.997	3.66	5.86	5.95	3.151	1.106	4.049	3.38
	2.19[a]	6.6[a]		6.5[a]	4.0[a]	3.12[a]	1.05[a]		
100	2.211	6.976	3.63	5.82	5.75	3.150	1.103	4.000	3.44
50	2.207	6.917	3.58	5.73	5.21	3.148	1.095	3.868	3.60
40	2.204	6.875	3.54	5.67	4.85	3.146	1.090	3.777	3.71
35	2.201	6.841	3.50	5.62	4.55	3.145	1.085	3.704	3.80
30	2.197	6.788	2.61	5.54	4.12	3.143	1.078	3.595	3.93
25	2.191	6.703	2.54	5.43	3.48	3.140	1.067	3.430	4.12
20	2.179	6.553	2.41	5.23	2.48	3.134	1.048	3.165	4.41
15	2.154	6.246	2.12	4.88	0.964	3.122	1.010	2.714	4.86
10	2.088	5.445		4.22		3.088	0.922	1.417	4.96
7	1.973	4.129		3.82		3.026	0.799		
5	1.777	1.98				2.908	0.578		
4	1.578					2.776	0.289		
3	1.212					2.467			
2.5	0.907					2.151			
2	0.446					1.562			
1.8						1.171			
1.7						0.9117			

[a]Reference [24].

Table 5. Comparison of the ^{1}P° resonance energies (eV) of Li^+ with other theoretical and experimental results.

States		Present	CRM[a]	CRM[b]	R-matrix[c]	Experiment[c]	Experiment[d]
$2s2p_+$	^{1}P°(1)	150.26	150.26	150.28	150.31	150.31 ± 0.03	150.31 ± 0.02
$2s3p_-$	^{1}P°(2)	159.16	159.16	159.17			
$2s3p_+$	^{1}P°(3)	161.04	161.04	161.05	161.08	161.11 ± 0.03	161.07 ± 0.02
$2p3d$	^{1}P°(4)	162.03	162.025	162.04			
$2s4p_-$	^{1}P°(5)	163.19		163.20			
$2s4p_+$	^{1}P°(6)	163.92		163.94	163.97	164.00 ± 0.03	163.95 ± 0.03
$2p4d$	^{1}P°(7)	164.32		163,34			
$2s5p_-$	^{1}P°(8)	164.86		164.87			
$2s5p_+$	^{1}P°(9)	165.23		165.23	165.26	165.29 ± 0.03	165.27 ± 0.06
$2s2p_+$	^{3}P°(1)	146.98	146.98	146.99			
$2s3p_+$	^{3}P°(2)	159.82	159.82	159.83			
$2s3p_-$	^{3}P°(3)	160.03	160.03	160.04			
$2p3d$	^{3}P°(4)	161.73	161.73	161.74			
$2s4p_+$	^{3}P°(5)	163.40		163.41			
$2s4p_-$	^{3}P°(6)	163.57		163.58			
$2p4d$	^{3}P°(7)	164.18		164.19			
$2s5p_+$	^{3}P°(8)	164.96		164.97			
$2s5p_-$	^{3}P°(9)	165.06		165.07			

[a]Reference [24]; [b]reference [25]; [c]reference [2]; [d]reference [26].

Table 6. Comparison of the ^{1}P° resonance widths (meV) of Li^+ with other theoretical and experimental results.

States		Present	CRM[a]	CRM[b]	R-matrix[c]	Experiment[c]
$2s2p_+$	^{1}P°(1)	60.19	59.59	60.08	60.08	57 ± 3
$2s3p_-$	^{1}P°(2)	0.1594	0.1769	0.1604		
$2s3p_+$	^{1}P°(3)	19.039	17.96	19.02	19.03	21 ± 2
$2p3d$	^{1}P°(4)	0.1618	0.1088	0.1605		
$2s4p_+$	^{1}P°(5)	9.959		8.40	8.39	6 ± 2
$2s2p_+$	^{3}P°(1)	8.574	8.49	8.792		
$2s3p_+$	^{3}P°(2)	3.009	2.86	3.093		
$2s3p_-$	^{3}P°(3)	0.092		0.09274		
$2s4p_+$	^{3}P°(5)	1.102		1.238		

[a]Reference [24]; [b]reference [25]; [c]reference [2].

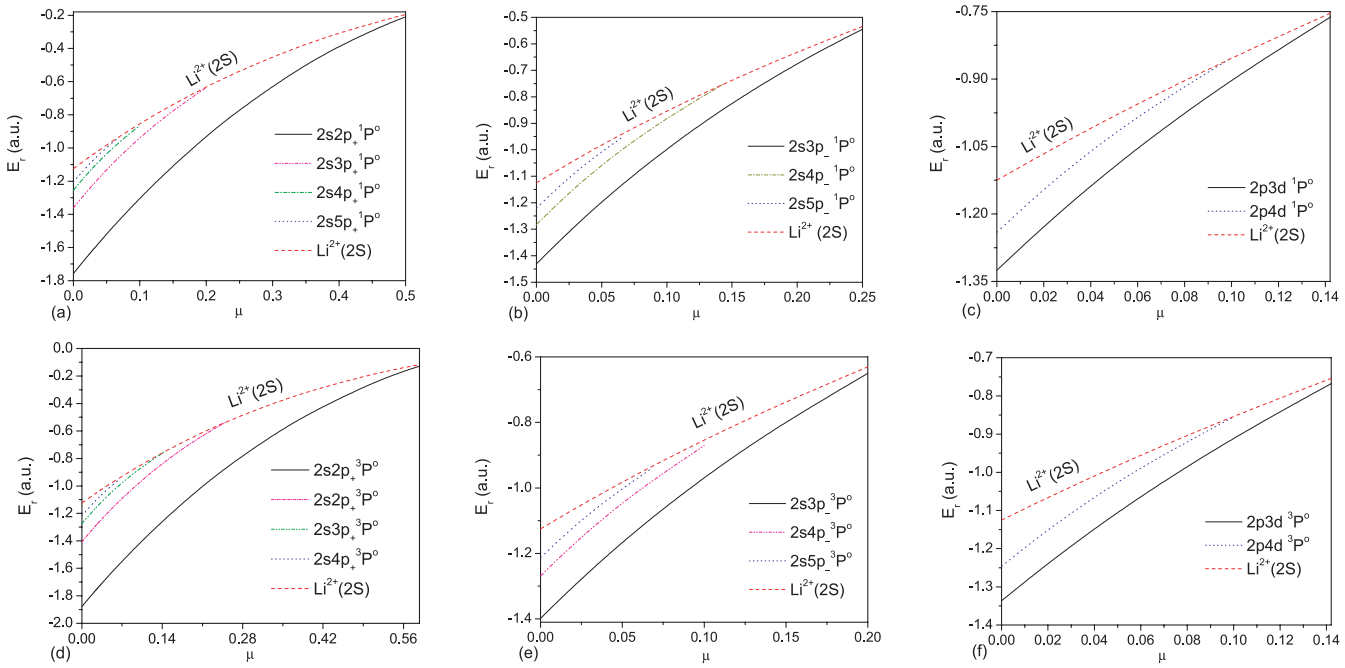

Fig. 3. The $2ln'l'$ $(2 \leq n' \leq 5)$ ^{1,3}P° resonance energies in terms of the screening parameter μ along with the Li^+ (2S) threshold energies.

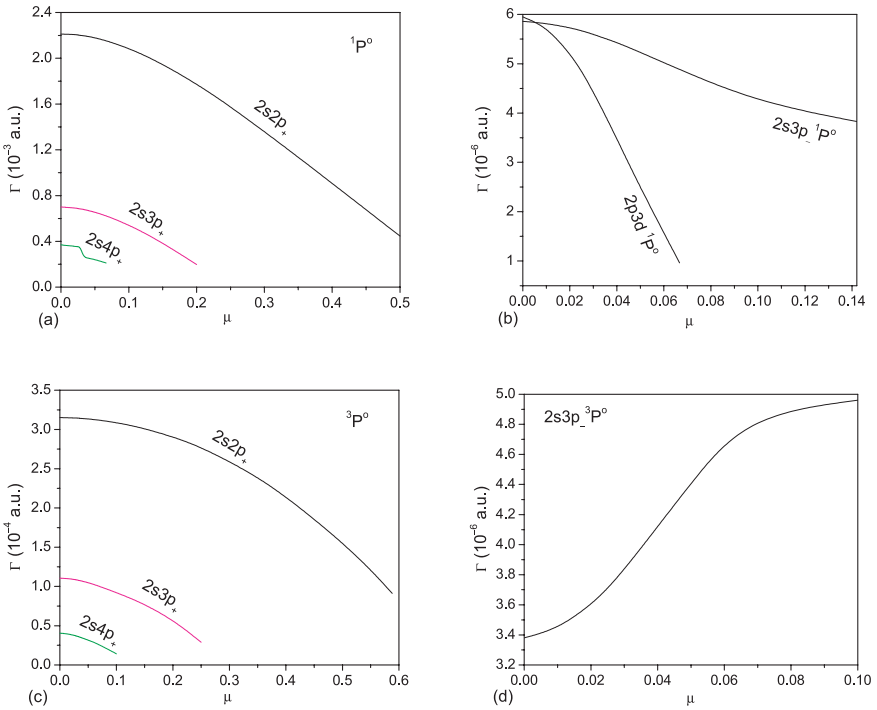

Fig. 4. The $2ln'l'$ $(2 \leq n' \leq 4)$ ^{1,3}P° resonance widths corresponding to resonance energies in Figure 3 as functions of the Debye screening parameter μ.

Table 7. The wavelengths (in Å) for the absorption ^{1}P° resonances of Li^+ in plasmas.

D	$2s2p_+$ ^{1}P°(1)	$2s3p_+$ ^{1}P°(3)	$2s4p_+$ ^{1}P°(6)	$2s5p_+$ ^{1}P°(9)	$2s3p_-$ ^{1}P°(2)	$2s4p_-$ ^{1}P°(5)	$2s5p_-$ ^{1}P°(8)	$2p3d$ ^{1}P°(4)	$2p4d$ ^{1}P°(7)
∞	82.507	76.985	75.630	75.03	77.894	75.971	75.20	76.516	75.446
100	82.512	76.995	75.645	75.05	77.902	75.984	75.22	76.525	75.462
50	82.528	77.022	75.689	75.11	77.925	76.021	75.27	76.552	75.506
30	82.564	77.085	75.786	75.25	77.978	76.107	75.40	76.615	75.606
20	82.633	77.203	75.967	75.49	78.080	76.266	75.62	76.732	75.792
15	82.729	77.364	76.207	75.8	78.218	76.479	75.92	76.892	76.04
10	82.995	77.806	76.85		78.600	77.054		77.332	76.71
7	83.478	78.595			79.285	78.055		78.139	
5	84.358	80.021			80.527				
4	85.344				81.929				
3	87.444								
2.5	89.554								
2	93.549								
1.8	96.5								

very close to the Li^+(2S) threshold with increasing plasma strength, i.e., with increasing value of the screening parameter μ, and all the resonance widths decrease with the increase of plasma strength except for the $2s3p_-$ ^{3}P° states. The $2s3p_-$ ^{3}P° resonance width increases with increasing plasma strength. All the situations have been discussed in our earlier works. From Figure 4c and Table 4, it is apparent that the resonance width for the $2s4p_+$ ^{1}P° state fall down slightly near $D = 30$. It may due to some numerical uncertainties during the fitting procedure using equation (5), or it may due to the finite basis sets we have used here. More extensive calculations in the future may help to clarify the sudden drop of the width for the $2s4p_+$ ^{1}P° state when μ is around 1/30. In Tables 2–4, the number in the first parenthesis indicates the order of appearance of resonance parameters and in Table 4, the exponent like 10^{-x} in the square bracket indicates the entry of each column should be multiplied by 10^{-x}.

5 Transition wavelengths

It is well-known that at energies close to resonance, the photo-ionization process for a positive ion Q^+ occurs as follows

$$\hbar\nu + Q^+(i) \rightarrow [Q^+]^{**} \rightarrow Q^{++}(f) + e^-, \qquad (6)$$

where $[Q^+]^{**}$ is an intermediate resonance state and i, f denote the initial and final states, respectively. The interference between the direct and the intermediate mechanisms in equation (6) yields the absorption profile. In the He-like Li^+ ion, the strongest process occurs for the final state $2snp(n \geq 2)$ ^{1}P° and the initial state $1s^2$ ^{1}S.

Finally in Table 7 and Figure 5, we present the transition wavelengths λ(Å)of the ^{1}P° absorption resonances from the ground state of the plasma-embedded Li^+ ion with various Debye lengths.

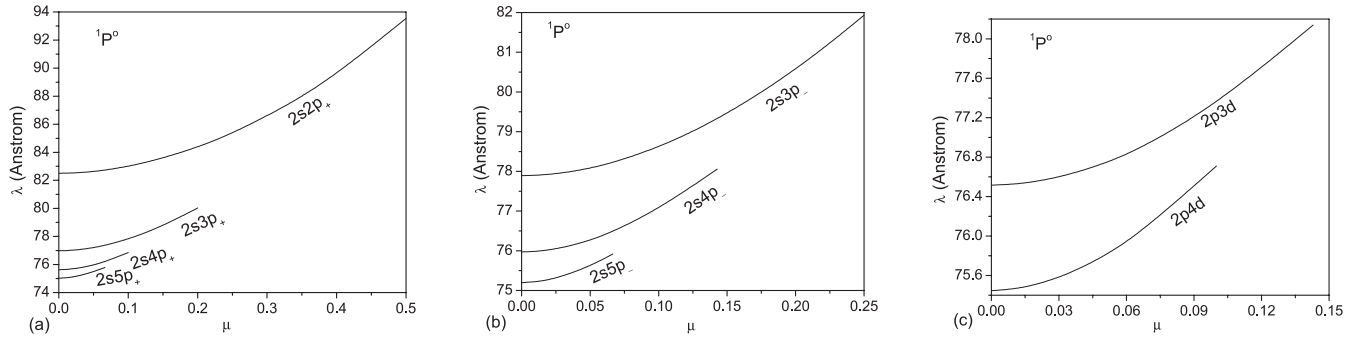

Fig. 5. The wavelengths for the absorption ^{1}P° resonances for the $2snp_+$ in (a), the $2snp_-$ in (b), the $2pnd$ in (c) of Li^+ in plasmas for different screening parameters.

To obtain the wavelengths, we first calculate the energy differences in atomic units between each of the autoionization $2ln'l'$ ($n' \geq 2$) ^{1}P° states and the ground $1s^2$ ^{1}S state of the Li^+ ion for different Debye lengths. The energy differences are then converted from atomic units to Angstrom (Å) by using the standard conversion unit (1 atomic unit of energy corresponds to a wavelength of 455.633 Å). Our results show that as the plasma screening effect increases, the wavelengths for the photo-absorption from the ground state to the doubly excited resonance states are red-shifted to have longer wavelengths (see Fig. 5).

6 Summary and conclusions

In view of the recent experimental measurement on the doubly excited resonances in photo-ionization spectrum of Li^+ [2], we have made a first investigation on the $2snp_+$ ($3 \leq n \leq 5$), $2snp_-$ ($3 \leq n \leq 5$), $2pnd$ ($n = 3, 4$) ^{1,3}P° resonance states of the Li^+ ion embedded in Debye plasma environments. We have also calculated the ground $1s^2$ ^{1}S state energies of the Li^+ ion in plasmas. The ground state energies and the resonance parameters (E_r, Γ) for various Debye lengths ranging from infinity (free ion, no screening) to small values (up to 1.7) have been calculated. Our ground state energies obtained for different screening parameters are lower than those reported in the literature. We have also estimated, for the first time, the wavelengths of absorption resonances for the Li^+ ion in plasmas under various Debye environments. We have employed the stabilization method that is a very simple and powerful practical method to calculate the resonance parameters (E_r, Γ). Our results will provide useful references to research communities in atomic physics, plasma physics, and astrophysics.

The work is supported by the National Science Council of R.O.C.

References

1. S. NaKai, K. Mima, Rep. Prog. Phys. **67**, 321 (2004)
2. S.W.J. Scully et al., J. Phys. B **39**, 3957 (2006)
3. P. Winkler, Phys. Rev. E **53**, 5517 (1996)
4. X. Lopez, C. Sarasola, J.M. Ugalde, J. Phys. Chem. **101**, 1804 (1997)
5. S.-T. Dai, A. Solovyova, P. Winkler, Phys. Rev. E **64**, 016408 (2001)
6. B. Saha, T.K. Mukherjee, P.K. Mukherjee, G.H.F. Diercksen, Theor. Chem. Acc. **108**, 305 (2002)
7. P.K. Mukherjee, J. Karwowski, G.H.F. Diercksen, Chem. Phys. Lett. **363**, 323 (2002)
8. B. Saha, T.K. Mukherjee, P.K. Mukherjee, Chem. Phys. Lett. **373**, 218 (2003)
9. S. Kar, Y.K. Ho, Chem. Phys. Lett. **402**, 544 (2005); S. Kar, Y.K. Ho, New J. Phys. **7**, 141 (2005)
10. H. Okutsu, T. Sako, K. Yamanouchi, G.H.F. Diercksen, J. Phys. B **38**, 917 (2005)
11. S. Kar, Y.K. Ho, Int. J. Quantum Chem. **106**, 814 (2006); S. Kar, Y.K. Ho, Int. J. Quantum Chem. **107**, 353 (2007)
12. S. Kar, Y.K. Ho, Phys. Rev. E **70**, 066411 (2004); S. Kar, Y.K. Ho, Phys. Rev. A **71**, 052503 (2005); S. Kar, Y.K. Ho, Phys. Rev. A **72**, 010703 (2005); S. Kar, Y.K. Ho, Phys. Rev. A **73**, 0 32502 (2006); S. Kar, Y.K. Ho, J. Phys. B **39**, 2455 (2006)
13. A.N. Sil, P.K. Mukherjee, Int. J. Quantum Chem. **102**, 1061 (2005)
14. S. Kar, Y.K. Ho, Chem. Phys. Lett. **424**, 403 (2006)
15. G.J. Iafrate, L.B. Mendelsohn, Phys. Rev. **182**, 244 (1969)
16. S. Ichimaru, in *Plasma Physics* (The Benjamin/Cummings Publishing Company, Inc., Menlo Park, California, 1986)
17. H.R. Griem, in *Principles of Plasma Spectroscopy* (Cambridge University Press, 2005)
18. V.A. Mandelshtam, T.R. Ravuri, H.S. Taylor, Phys. Rev. Lett. **70**, 1932 (1993)
19. S.S. Tan, Y.K. Ho, Chin. J. Phys. **35**, 701 (1997)
20. S. Kar, Y.K. Ho, J. Phys. B **38**, 3299 (2005); S. Kar, Y.K. Ho, J. Phys. B **37**, 3177 (2004); S. Kar, Y.K. Ho, Eur. Phys. J. D **35** 453 (2005); U. Roy, Y. K Ho, Nucl. Instr. Meth. B **221**, 36 (2004); U. Roy, Y. K Ho, J. Phys. B **35**, 2149 (2002); Z.-C. Yan, Y.K. Ho, J. Phys. B **36**, 4417 (2003); T.K. Fang, Y.K. Ho, J. Phys. B **32**, 3863 (1999); W.J. Pong, Y.K. Ho, J. Phys. B **31**, 2177 (1998)
21. A.M. Frolov, Phys. Rev. E **64**, 036704 (2001)
22. A.M. Frolov, V.H. Smith Jr, J. Phys. B **37**, 2917 (2004)
23. F.J. Rogers, H.C. Grabsoke Jr, D.J. Harwood, Phys. Rev. A **1**, 1577 (1970)
24. Y.K. Ho, Phys. Rev. A **23**, 2137 (1981)
25. K.T. Chung, C.D. Lin, At. Mol. Data Tables **69**, 101 (1998)
26. J.-P. Mosiner, J. Costello, E.T. Kennedy, W. Whitty, J. Phys. B **33**, 5203 (1999)